Effects of Ca^{2+}/calmodulin-dependent protein kinase pathway inhibitor KN93 on osteoclastogenesis

YINGXIAO FU[1*], DEQUN NIU[2*], WENFANG SU[2], QINGLING YANG[3], WENRUI WANG[1], BAODING TANG[1], ZHONGWEN LI[1], DING ZHANG[1], YINGJI MAO[1], CHUANG LI[1], XUE LI[1], SHIHAO YE[1], XU SU[1], FANYUAN XU[1], XUEMIN SUN[4] and CHANGJIE CHEN[1]

[1]Department of Bioscience, Bengbu Medical College; [2]Department of Gynecology and Obstetrics, The Second Affiliated Hospital of Bengbu Medical College; Departments of [3]Medical Laboratory and [4]Clinical Medicine, Bengbu Medical College, Bengbu, Anhui 233000, P.R. China

Received February 26, 2018; Accepted July 20, 2018

DOI: 10.3892/ijmm.2018.3793

Abstract. The aim of the present study was to determine the effects of the Ca^{2+}/calmodulin-dependent protein kinase pathway inhibitor KN93 on osteoclastogenesis. RAW264.7 cells were incubated with macrophage colony-stimulating factor (M-CSF) + receptor activator of nuclear factor kappa-light-chain-enhancer of activated B cells ligand (RANKL) to stimulate osteoclastogenesis and then treated with 10 μM KN93. The methods included tartrate-resistant acid phosphatase (TRAP) staining, bone resorption activity assays, filamentous (F)-actin staining, determination of intracellular calcium ($[Ca^{2+}]_i$) levels, monitoring of osteoclast-specific gene expression levels and measurement of key transcription factors protein levels. The results suggested that KN93 inhibited the formation of TRAP-positive multinucleated cells, shaping of F-actin rings and resorption activity of the cells. In addition, KN93 decreased the concentration of $[Ca^{2+}]_i$, expression levels of osteoclast specific genes and protein levels of critical transcription factors in the M-CSF + RANKL-induced osteoclast model. In summary, KN93 may directly affect the differentiation and activation of osteoclasts, potentially through the Ca^{2+}/calmodulin-dependent protein kinase signaling pathway.

Introduction

Multinucleated osteoclasts originate from bone marrow myeloid precursor cells and serve a major role in bone remodeling (1,2). Abnormally activated osteoclasts may give rise to osteosclerosis, osteoporosis, rheumatoid arthritis, Huppert's disease, periodontal disease and metabolic bone disorders (3). Therefore, sufficient understanding of the osteoclast differentiation mechanisms is crucial for the prevention and treatment of these diseases. Cytokines that mediate the differentiation and maturation of osteoclasts directly and/or indirectly regulate the expression of critical genes through complex signal transduction pathways. At present, the signal transduction terminal transcription factors including nuclear factor kappa-light-chain-enhancer of activated B cells (NF-κB), proto-oncogene c-Fos (c-Fos), Jun proto-oncogene (c-Jun) and nuclear factor of activated T-cells (NFAT) have been identified to be involved in these processes. Furthermore, these pathways have been demonstrated to interact with each other (4-6).

The Ca^{2+} signaling pathway exerts a dominative role in osteoclast differentiation and activation. Seales *et al* (7) and Berridge *et al* (8) suggested that Ca^{2+} oscillations occur in the process of receptor activator of NF-κB ligand (RANKL)-induced osteoclast formation. Calmodulin and its downstream factors are also activated by RANKL. Ca^{2+}/calcineurin, and calcineurin target NFAT, are the key regulators of osteoclast formation (7,8). Previous studies have indicated that Ca^{2+}/calmodulin dependent protein kinases (CaMKs) regulate the formation of osteoclasts via the activated transcription factor activator protein1 (AP-1), while the AP-1 family proteins members c-Fos and c-Jun are involved in the regulation of bone metabolism (7,9). In addition, CaMKs may inhibit the osteoclast differentiation by negatively regulating the glycoprotein 130 (gp130) receptor pathway in order to promote the formation of osteoclasts (7). RANKL initiates Ca^{2+} oscillations, which results in calcineurin-mediated activation of NFAT, cytoplasmic 1 (NFATC1) and ultimately promotes the formation of osteoclasts (10). KN93 is a CaMK inhibitor that lacks subtype specificity (11). It was demonstrated that the CaMKs inhibitor KN93 was involved in osteoclast differentiation, although the mechanism remains unknown (12-14).

Odanacatian is a Cathepsin K kinase inhibitor and Saraconine is an inhibitor of Src family kinases. These molecules are required for normal osteoclastic functions and were suggested to restrain osteoclast resorption activity (15-17). To the best of our knowledge, the investigation of the CaMKs

Correspondence to: Professor Changjie Chen, Department of Bioscience, Bengbu Medical College, 2600 Donghai Road, Bengbu, Anhui 233000, P.R. China
E-mail: BBMCosteoclast@outlook.com

*Contributed equally

Key words: Ca^{2+}/calmodulin-dependent protein kinase pathway, KN93, osteoclastogenesis

inhibitor KN93 as a biologically-active osteoclast inhibitor has not yet been described. Our previous study indicated that KN93 (10 ng/ml) effectively blocked CaMKs activation in osteoclasts (18). However, whether KN93 directly affects the differentiation and activation of osteoclasts remains unknown.

TRAP staining, bone resorption activity assays, filamentous (F)-actin staining, as well as the determination of intracellular calcium ($[Ca^{2+}]_i$) levels, osteoclast-specific gene expression levels monitoring and protein levels of important transcription factors protein levels, were investigated in the present study. The results suggested that KN93 inhibited the formation of TRAP-positive multinucleated cells, the shaping of F-actin rings and the resorption activity of the cells. Furthermore, the results revealed that KN93 decreased the intracellular concentrations of $[Ca^{2+}]_i$, expression levels of osteoclast-specific genes and protein expression levels of important transcription factors associated with the macrophage colony-stimulating factor (M-CSF) + RANKL-induced osteoclast model.

Materials and methods

Cell culture and KN93 treatment. The murine monocyte/macrophage RAW 264.7 cell line was obtained from the American Type Culture Collection (Manassas, VA, USA). The cells were incubated in Dulbecco's modified Eagle's medium (GE Healthcare, Chicago, IL, USA) containing 10% fetal bovine serum (FBS; GE Healthcare), 2 mM/l L-glutamine, 100 U/ml penicillin and 100 μg/ml streptomycin at 37˚C in a humidified atmosphere of 5% CO_2. In order to induce osteoclast differentiation, RAW264.7 cells were resuspended in minimum essential medium (MEM)-α (GE Healthcare) and seeded into 6-well plates ($5x10^4$ cells/ml) and cultured for 4 h at 37˚C in a humidified atmosphere of 5% CO_2. The medium was changed to MEM-α containing 25 ng/ml M-CSF + 30 ng/ml RANKL (PeproTech, Inc., Rocky Hill, NJ, USA) + dimethyl sulfoxide [(DMSO); control, KN93 was dissolved in DMSO), 25 ng/ml M-CSF + 30 ng/ml RANKL and 25 ng/ml M-CSF + 30 ng/ml RANKL + 10 μM KN93 (Sigma-Aldrich; Merck KGaA, Darmstadt, Germany) + DMSO. The cells were cultured for an additional 4 days.

Cell viability assay (MTT assay). To examine the effect of KN93 on cell growth, RAW264.7 cells were treated with various concentrations of KN93 and cell growth was measured by the MTT assay (Beijing Solarbio Science & Technology Co., Ltd., Beijing, China). In summary, the cells were plated in 96-well plates in MEM-α containing 10% FBS and cultivated for 4 h. Different concentrations of KN93 (1, 2, 5, 10 and 20 μM), and KN93 (1, 2, 5, 10 and 20 μM) + 25 ng/ml M-CSF + 30 ng/ml RANKL were added into the culture for an additional 96 h. At the end of the incubation, the plates were washed with PBS 3 times, and 100 μl 0.5 mg/ml MTT solution in PBS was added into each well. Following an overnight incubation at 37˚C, the insoluble formazan crystals were dissolved in 100 μl DMSO. Following 10 sec of shaking, the optical densities (OD) of the samples were immediately measured at 595 nm using a Sunrise microplate reader (Tecan Group, Ltd., Männedorf, Switzerland).

Osteoclast differentiation detection. Osteoclast differentiation was detected by counting cells positively stained by tartrate-resistant acid phosphatase (TRAP) using TRAP Acid Phosphatase kit 387-A (Sigma-Aldrich; Merck KGaA). TRAP staining was performed in accordance with the protocol provided by the manufacturer. The samples were monitored under a phase-contrast microscope (original magnification, x100) and TRAP-positive multinucleated (3 nuclei) cells were selected in five random visual fields in different areas of each well.

Osteoclast resorption activity assay. Osteoclast resorption activity was detected using the Corning Osteo Assay Surface (COAS; Corning Inc., Corning, NY, USA). RAW264.7 cells were seeded onto the COAS ($1.5x10^4$ cells/ml, 200 μl/well) and cultured at 37˚C in a humidified atmosphere of 5% CO_2 for 4 h. The medium used was MEM-α with or without KN93, and the cells were incubated at 37˚C in a humidified atmosphere of 5% CO_2 for 4 days. The operating methods were based on the manufacturer's protocol, as described previously (19). The resorbing lacunae appeared as single or multiple clusters on the bottom of the COAS wells and were visualized under an inverted phase contrast microscope (original magnification, x 100). A total of five visual fields were selected randomly and counted in each sample. The resorption area was measured using morphological microscopic image analysis system (version 1.0; Shenzhen Jeda Technology Development Co., Ltd., Shenzhen, China).

F-actin staining. Tetramethylrhodamine (TRITC)-conjugated phalloidin (20 μM; Invitrogen; Thermo Fisher Scientific, Inc., Waltham, MA, USA) was employed to stain the F-actin cytoskeleton. RAW264.7 cells were resuspended in MEM-α, seeded into 24-well plates and cultured for 4 h at 37˚C in a humidified atmosphere of 5% CO_2. Following this, the medium was replaced with MEM-α containing 25 ng/ml M-CSF + 30 ng/ml RANKL+ DMSO, 25 ng/ml M-CSF + 30 ng/ml RANKL or 25 ng/ml M-CSF + 30 ng/ml RANKL + 10 μM KN93 + DMSO. Cells were then cultured for an additional 4 days at 37˚C in a humidified atmosphere of 5% CO_2. Then medium was discarded, and the cells were fixed with 4% paraformaldehyde solution for 10 min at room temperature, permeabilized by 0.1% Triton X-100, and stained for 20 min at room temperature according to the manufacturer's protocol. The stained cells were observed under an inverted phase contrast fluorescence microscope (original magnification, x100) (DMI 3000B; Leica Microsystems GmbH, Wetzlar, Germany).

$[Ca^{2+}]_i$ concentration quantification by flow cytometry. RAW264.7 cells were resuspended in MEM-α and seeded into 24-well plates and cultured for 4 h at 37˚C in a humidified atmosphere of 5% CO_2. The medium was changed to MEM-α containing 25 ng/ml M-CSF + 30 ng/ml RANKL+ DMSO, 25 ng/ml M-CSF + 30 ng/ml RANKL and 25 ng/ml M-CSF + 30 ng/ml RANKL + 10 μM KN93 + DMSO. The cells were cultured for an additional 4 days. Following this, the medium was discarded, and the plates were washed with PBS three times in order to remove the FBS and the phenol red in the cell culture medium. The cells were collected and transferred to

microcentrifuge tubes. A total of 400 μl Fluo-4-AM (Dojindo Molecular Technologies, Inc., Kumamoto, Japan) was added to a final concentration of 5 μM. The cells were incubated in the dark for 30 min at 37˚C and rinsed three times with PBS. A total of 400 μl PBS was added to the microcentrifuge tubes. The cells were resuspended and incubated for 30 min at 37˚C in a thermostatic water bath. The mean fluorescent intensity from $1x10^4$ randomly selected cells was measured using a flow cytometer (Accuri C6, BD Biosciences, Franklin Lakes, NJ, USA) at an emission wavelength of 516 nm with alternate excitation wavelengths of 494 nm. The results were analyzed by FlowJo 7.6 software (TreeStar, Inc., Ashland, OR, USA).

Reverse transcription quantitative polymerase chain reaction (RT-qPCR) analysis of TRAP, Cathepsin K, and matrix metalloproteinase (MMP)-9 mRNA levels. RAW264.7 cells were resuspended in MEM-α at a density of $5x10^4$ cells/ml and then seeded into 6-well culture plates at a volume of 2 ml/well. Following 4 h of culture, the medium was changed to MEM-α with or without KN93 and the cells were cultured for an additional 96 h at 37˚C in a humidified atmosphere of 5% CO_2. Total RNA was extracted using a Total RNA Kit I (Omega Bio-Tek, Inc., Norcross, GA, USA) and cDNA synthesis was conducted with 2 μg RNA using the RevertAid First strand cDNA Synthesis kit (Thermo Fisher Scientific, Inc.). The Real-time PCR SYBR Premix Dimer Eraser kit was purchased from Takara Bio., Inc. (Otsu, Japan), and qPCR was performed using the Q6 Flex Real Time PCR system (Applied Biosystems; Thermo Fisher Scientific, Inc.). The qPCR thermocycling conditions used for TRAP were as follows: 95˚C for 30 sec; followed by 40 cycles of 57˚C for 1 min; and finally 72˚C for 34 sec. The qPCR thermocycling conditions used for MMP-9 were as follows: 95˚C for 30 sec; followed by 40 cycles of 55.6˚C for 1 min; 72˚C for 34 sec. The qPCR thermocycling conditions used for Cathepsin K were as follows: 95˚C for 30 sec; followed by 40 cycles of 56.8˚C for 1 min; and finally 72˚C for 34 sec. The specificity of the PCR products was verified by melting curve analysis. The $2^{-\Delta\Delta Cq}$ method was used to analyze relative gene expression data (20). The specific sequences of the PCR primers for TRAP, MMP-9, Cathepsin K and GAPDH were as follows: TRAP forward 5'-GGCTAC TTGCGGTTTCACTAT-3'; TRAP reverse 5'-TCCTTGGGA GGCTGGTCT-3'; MMP-9 forward 5'-GCCCTGGAACTC ACACGACA-3'; MMP-9 reverse 5'-TTGGAAACTCACACG CCAGAAG-3'; Cathepsin K forward 5'-CGCCTGCGGCAT TACCAA-3'; Cathepsin K reverse 5'-TAGCATCGCTGC GTCCCT-3'; GAPDH forward 5'-AAATGGTGAAGGTCG GTGTG-3' and GAPDH reverse 5'-TGAAGGGGTCGTTGA TGG-3'.

SDS-PAGE and western blot analysis. Cultured cells were collected and lysed in 100 μl radioimmunoprecipitation assay (Beyotime Institute of Biotechnology, Haimen, China) buffer with 1 μl phenylmethyl sulphonyl fluoride for 30 min on ice. Following ultrasonic disruption (at 4˚C, 2x10 sec and 20 kHz), the lysed cells were centrifuged (12,000 x g for 15 min at 4˚C) and the supernatants containing the total protein were collected. The concentration of total protein was determined by a bicinchoninic acid Protein Assay kit (Beyotime Institute of Biotechnology) for each sample, and equal amounts (50 μg) were separated on 12% SDS-PAGE gels at 110 V for 120 min. The separated protein bands were transferred by electroblotting to nitrocellulose filter membranes (Beyotime Institute of Biotechnology). The membranes were blocked in Blocking buffer (Beyotime Institute of Biotechnology) for 60 min at room temperature. The membranes were incubated overnight at 4˚C with primary anti-c-Fos (1:1,000; cat. no. 2250S), anti-phosphorylated (phospho)-c-Fos (1:1,000; cat. no. 5348S), anti-c-Jun (1:1,000; cat. no. 9165S), anti-phospho-c-Jun (1:1,000; cat. no. 3270S), anti-NFATC1 (1:1,000; cat. no. 8032S) (all from Cell Signaling Technology, Inc., Danvers, MA, USA), and anti-β-actin antibodies (1:1,000; cat. no. sc-47778; Santa Cruz Biotechnology, Inc., Dallas, TX, USA). The antibodies were diluted in primary antibody dilution buffer (Beyotime Institute of Biotechnology). The membranes were incubated at room temperature for 60 min with goat anti-rabbit IgG-horseradish peroxidase (HRP) secondary antibody (cat. no. sc-2357; Santa Cruz Biotechnology, Inc.). The antibodies were diluted (1:5,000) by secondary antibody dilution buffer (Beyotime Institute of Biotechnology). The immunoreactive proteins were visualized by electrochemiluminescence using Immobilon Western Chemiluminescent HRP Substrate Detection reagent (EMD Millipore, Billerica, MA, USA). The gray levels of the protein bands were evaluated by Bio-Rad image lab analyzer v.5.2 software (Bio-Rad Laboratories, Inc., Hercules, CA, USA).

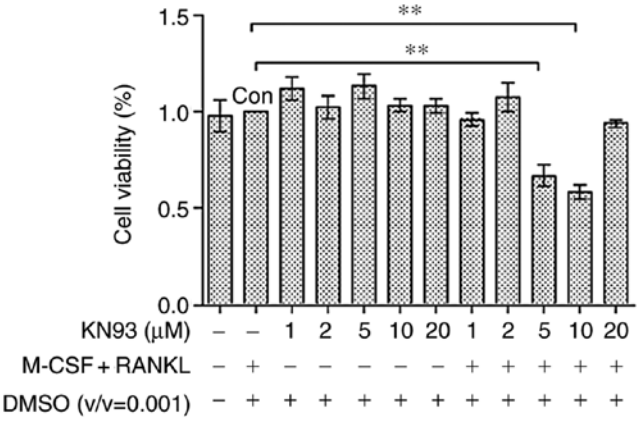

Figure 1. Effect of KN93 on cell viability is determined by MTT assay. The results are presented as mean ± standard error of the mean. **P<0.01 vs. con. Con, vehicle-treated cells; M-CSF, macrophage colony-stimulating factor; RANKL, receptor activator of nuclear factor kappa-light-chain-enhancer of activated B cells ligand; DMSO, dimethyl sulfoxide.

Statistical analysis. All experiments were repeated in triplicate and the data are presented as the mean ± standard error of the mean. Statistical differences between groups were evaluated by analysis of variance followed by a Tukey's post-hoc test using SPSS v.17.0 software (SPPS, Inc., Chicago, IL, USA). P<0.05 was considered to indicate a statistically significant difference.

Results

KN93 affects cell viability. KN93 did not affect RAW 264.7 cell growth rate (Fig. 1), sustaining substantial

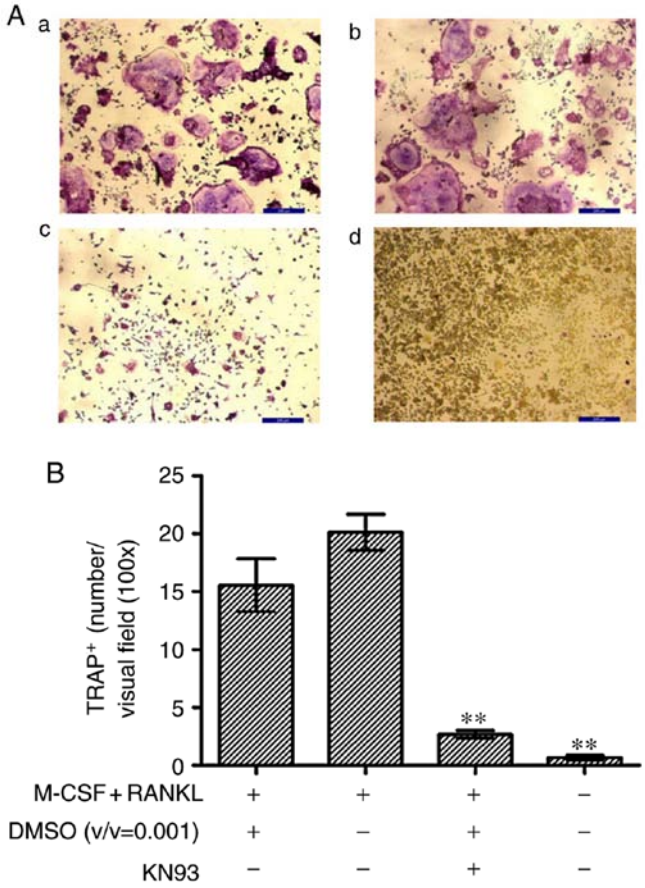

Figure2.KN93inhibitsosteoclastdifferentiationinM-CSF+RANKL-stimulated RAW 264.7 cells. (A) M-CSF (25 ng/ml) + RANKL (30 ng/ml) with or without 10 μM KN93 was added to RAW 264.7 cells. Following 96-h incubation, cells were stained with TRAP and images were captured. a, M-CSF + RANKL + DMSO; b, M-CSF + RANKL; c, M-CSF + RANKL + DMSO + KN93; and d, RAW264.7 cells. (B) TRAP+ multinucleated cells were counted and compared. The results are expressed as mean ± standard error of the mean. **P<0.01 vs. M-CSF + RANKL-stimulated RAW 264.7 cells. Original magnification, x100. Scale bar=200 μm. M-CSF, macrophage colony-stimulating factor; RANKL, receptor activator of nuclear factor kappa-light-chain-enhancer of activated B cells ligand; DMSO, dimethyl sulfoxide; TRAP, tartrate-resistant acid phosphatase; TRAP$^+$, TRAP-positive.

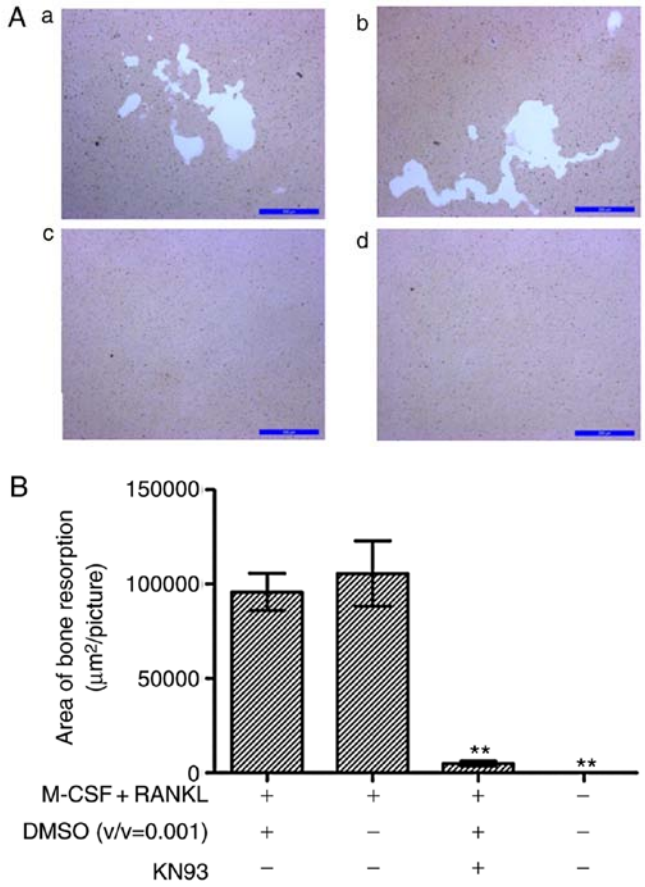

Figure 3. KN93 inhibits bone-resorbing ability of osteoclasts. (A) M-CSF + RANKL-treated RAW 264.7 cells were cultured in the presence and/or absence of 10 μM KN93. Following culturing, resorption lacunae were observed and images were captured. a, M-CSF + RANKL + DMSO; b, M-CSF + RANKL; c, M-CSF + RANKL + DMSO + KN93; and d, RAW264.7 cells. (B) Resorption lacunae area were calculated and compared. The results are presented as mean ± standard error of the mean. **P<0.01 vs. M-CSF + RANKL-stimulated RAW 264.7 cells. Original magnification, x100. Scale bar=200 μm. M-CSF, macrophage colony-stimulating factor; RANKL, receptor activator of nuclear factor kappa-light-chain-enhancer of activated B cells ligand; DMSO, dimethyl sulfoxide.

viability even at concentrations of 20 μM (102.95%). The data demonstrated that KN93 was not cytotoxic to RAW264.7 cells. However, KN93 affected the cell growth rate of 25 ng/ml M-CSF + 30 ng/ml RANKL-treated RAW 264.7 cells at concentrations of 5 μM (66.79%) and 10 μM (58.19%). Therefore, the concentrations of 10 μM KN93 + 25 ng/ml M-CSF + 30 ng/ml RANKL were used in subsequent experiments.

KN93 suppresses the formation of TRAP-positive multinucleated cells. RAW 264.7 cells were treated with M-CSF + RANKL for 96 h and then differentiated into TRAP-positive multinucleated cells (Fig. 2A). There was no significant difference between the number of TRAP-positive cells in the M-CSF + RANKL group (20.11±2.69), and in the KN93 (in DMSO) + M-CSF + RANKL group (15.55±3.98). Concomitantly, 10 μM KN93 + M-CSF + RANKL significantly suppressed osteoclast differentiation (2.66±0.58), as indicated in Fig. 2B. The number of TRAP-positive cells between M-CSF + RANKL group and the KN93 + M-CSF + RANKL group was significantly different (P<0.01).

KN93 inhibits the activation of osteoclasts. The effect of KN93 on M-CSF + RANKL-induced osteoclast activation was additionally examined. RAW 264.7 cells were stimulated with M-CSF + RANKL in order to induce differentiation into functionally-active osteoclasts with bone-resorbing capacities. The lacunae were shaped on the bottoms of the COAS in the M-CSF + RANKL and the DMSO + M-CSF + RANKL groups, whereas pit formation was evident in the KN93 + M-CSF + RANKL group (Fig. 3A). The resorption lacunae area is presented in Fig. 3B. The area of the KN93 + M-CSF + RANKL group (4,978.26±2,270.20 μm^2) was significantly decreased compared with that of the M-CSF + RANKL group (105,653.3±30,017.07 μm^2) (P<0.01).

Effect of KN93 on the F-actin shape in M-CSF + RANKL-treated RAW264.7 cells. The results revealed that

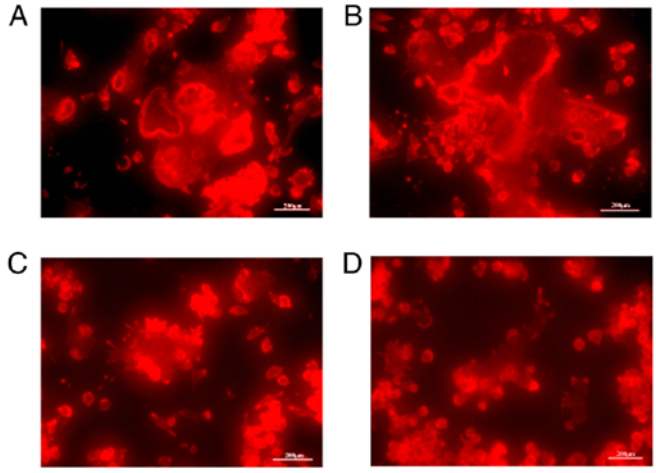

Figure 4. KN93 affects F-actin ring formation in M-CSF + RANKL-treated RAW264.7 cells. M-CSF + RANKL-treated RAW 264.7 cells were cultured in the presence and/or absence of 10 μM KN93. Following culture, TRITC-conjugated phalloidin staining was conducted, and F-actin rings were observed. (A) M-CSF + RANKL + DMSO. (B) M-CSF + RANKL. (C) M-CSF + RANKL + DMSO + KN93. (D) RAW264.7 cells. Original magnification, x100. Scale bar=200 μm. M-CSF, macrophage colony-stimulating factor; RANKL, receptor activator of nuclear factor kappa-light-chain-enhancer of activated B cells ligand; DMSO, dimethyl sulfoxide; TRITC, tetramethylrhodamine.

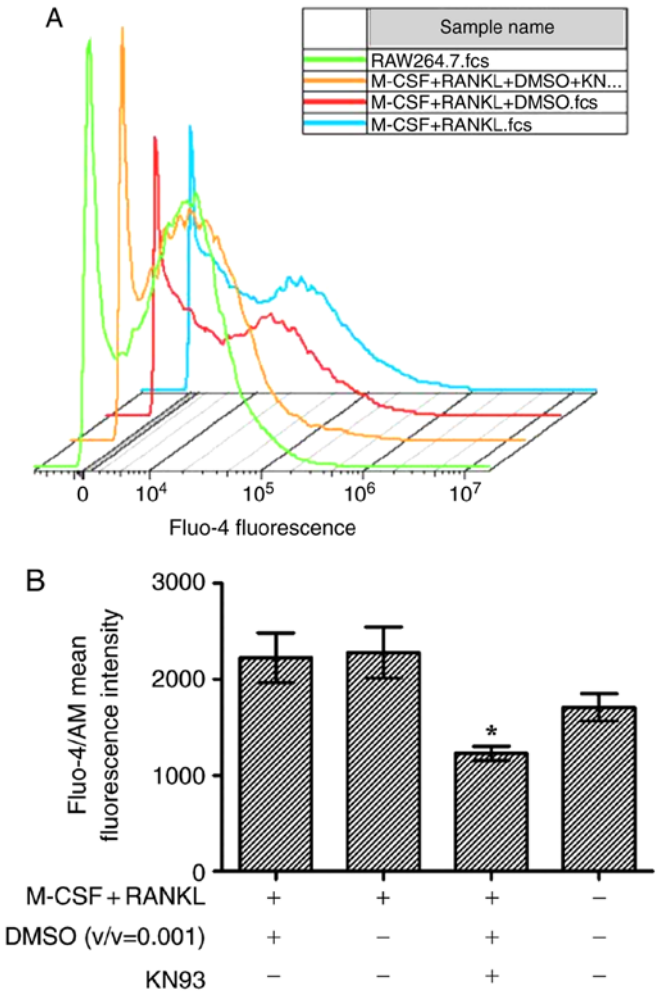

Figure 5. KN93 affects concentration of $[Ca^{2+}]_i$ in differentiated osteoclasts. (A) M-CSF + RANKL-treated RAW 264.7 cells were cultured in the presence and/or absence of 10 μM KN93. Following culture, fluorescence intensity of Fluo-4-AM was determined by flow cytometry. (B) The fluorescence intensities were compared. The results are presented as mean ± standard error of the mean. *P<0.05 vs. M-CSF + RANKL-stimulated RAW 264.7 cells. M-CSF, macrophage colony-stimulating factor; RANKL, receptor activator of nuclear factor kappa-light-chain-enhancer of activated B cells ligand; DMSO, dimethyl sulfoxide.

intact and regular F-actin rings were evident in the M-CSF + RANKL + DMSO group (Fig. 4A). Additionally, in the M-CSF + RANKL-treated cell population, the majority of differentiated osteoclasts were characterized by cells with a rounded morphology that contained clearly visible F-actin rings (Fig. 4B). Nevertheless, treatment with 10 μM KN93 inhibited the formation of F-actin rings in the M-CSF + RANKL-treated RAW264.7 cells (Fig. 4C).

KN93 affects the levels of $[Ca^{2+}]_i$ in osteoclast differentiation. The concentration of $[Ca^{2+}]_i$ was indirectly elucidated according to the fluorescence intensity of Fluo-4-AM. No significant difference in the concentration of $[Ca^{2+}]_i$ in M-CSF + RANKL-induced RAW264.7 cells compared with M-CSF + RANKL + DMSO-treated cells was observed. Concomitantly, the level of $[Ca^{2+}]_i$ in the M-CSF + RANKL + DMSO + KN93 group was significantly decreased compared with that of the M-CSF + RANKL group (P<0.05; Fig. 5).

TRAP, MMP-9 and Cathepsin K expression in KN93 + M-CSF + RANKL-treated osteoclast cells The gene expression levels of TRAP, MMP-9 and Cathepsin K were examined by RT-qPCR. No significant difference in the expression levels of TRAP, MMP-9 and Cathepsin K mRNA between the M-CSF + RANKL + DMSO and the M-CSF + RANKL groups was observed. Furthermore, the expression levels of TRAP in the M-CSF + RANKL + DMSO + KN93-treated cells were significantly decreased compared with the M-CSF + RANKL groups (P<0.05). The expression levels of MMP-9 in the M-CSF + RANKL + DMSO + KN93-treated cells were significantly decreased compared with the M-CSF + RANKL groups (P<0.05). The expression levels of Cathepsin K in the M-CSF + RANKL + DMSO + KN93-treated cells were significantly decreased compared with the M-CSF + RANKL groups (P<0.01). Treatment of the cells with 10 μM KN93 decreased the expression levels of TRAP, MMP-9 and Cathepsin mRNA to 0.57±0.07, 0.34±0.16 and 0.97±0.05-fold, respectively, compared with the M-CSF + RANKL groups (Fig. 6).

Effects of KN93 on the expression of osteoclast-specific transcription factors. NFAT c1 (NFATc1), and AP-1 protein family members c-Jun and c-Fos are considered to be the most crucial osteoclast-specific transcription factors (21). The present study examined whether these transcription factors were modulated by KN93 using western blot analysis. Treatment of RAW264.7 cells with 10 μM KN93 + M-CSF + RANKL significantly decreased the M-CSF + RANKL-stimulated upregulation of the NFATc1, p-C-Jun, and p-C-Fos transcription factors compared with the M-CSF + RANKL-treated cells (Fig. 7).

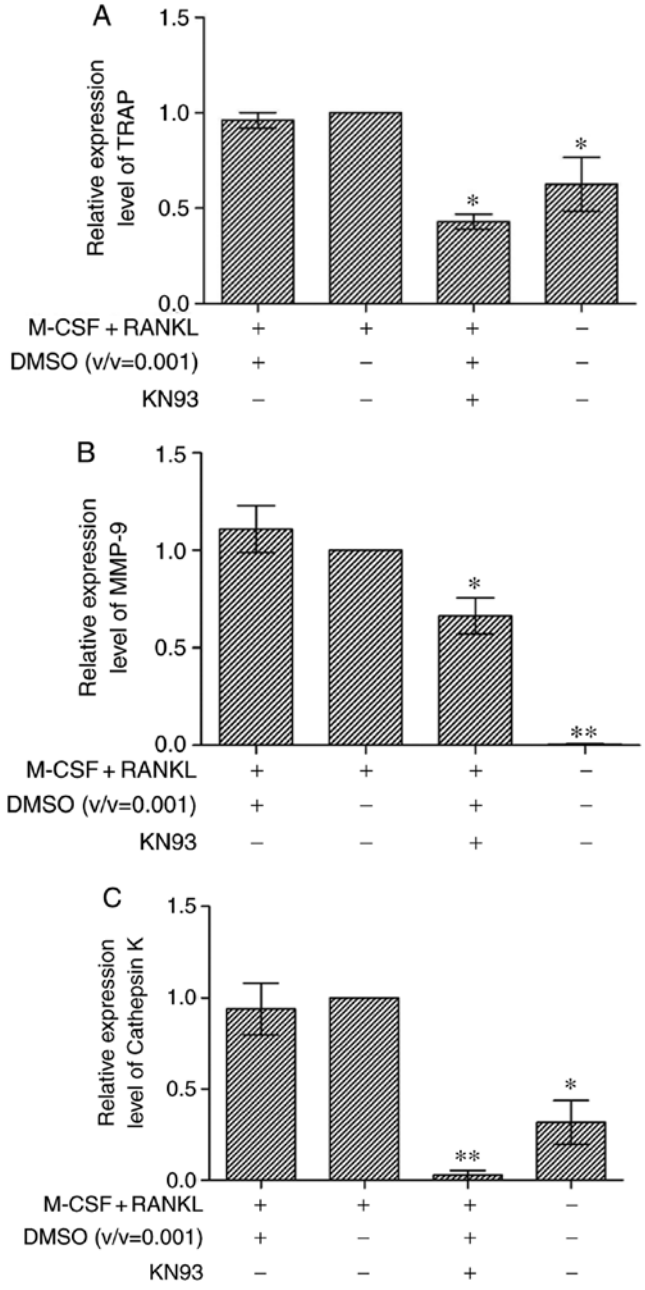

Figure 6. Effect of KN93 on the expression of TRAP, MMP-9 and Cathepsin K genes. RAW264.7 cells were cultured in minimum essential medium-α, and then seeded in 6-well culture plates. After 4 h of culture, M-CSF + RANKL with or without KN93 were added. Following additional culture steps, total RNA were collected, and mRNA expression levels of (A) TRAP, (B) MMP-9 and (C) Cathepsin K genes were measured. The results are expressed as mean ± standard error of the mean. *P<0.05 and **P<0.01 vs. M-CSF + RANKL groups. M-CSF, macrophage colony-stimulating factor; RANKL, receptor activator of nuclear factor kappa-light-chain-enhancer of activated B cells ligand; DMSO, dimethyl sulfoxide; TRAP, tartrate-resistant acid phosphatase; MMP-9, matrix metalloproteinase 9.

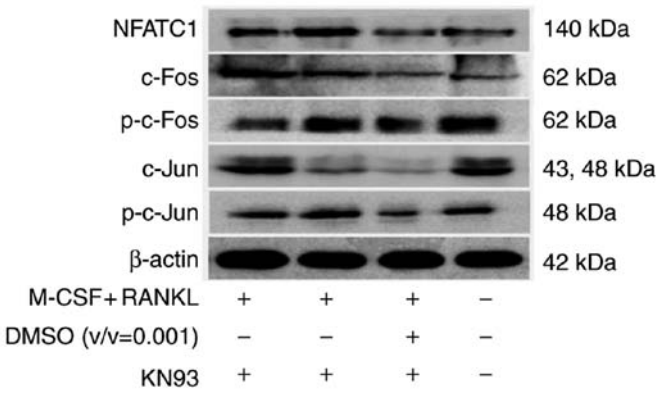

Figure 7. KN93 downregulates the expression of osteoclast-specific transcription factors in M-CSF + RANKL-stimulated RAW264.7 cells. RAW264.7 cells were cultured in the presence of M-CSF + RANKL, and with or without 10 μM KN93. Following culture for 96 h, total proteins were extracted and equal amount of proteins were assayed by western blot analysis. NFATC1, nuclear factor of activated T-cells, cytoplasmic 1; c-Fos, proto-oncogene c-Fos; p, phosphorylated; c-Jun, Jun proto-oncogene; M-CSF, macrophage colony-stimulating factor; RANKL, receptor activator of nuclear factor kappa-light-chain-enhancer of activated B cells ligand; DMSO, dimethyl sulfoxide.

Discussion

M-CSF is critical in the survival and differentiation of osteoclast precursor cells. M-CSF exerts its anti-apoptotic function via the anti-apoptotic gene B-cell lymphoma 2 (Bcl-2). M-CSF may act through the stimulation of extracellular signal regulated kinase (ERK) via growth factor receptor bound protein 2, and the activation of protein kinase B (Akt) by the phosphatidylinositol 3-kinase pathway and consequent promotion of osteoclast precursor cell survival (22,23). In addition, M-CSF may induce the expression of RANK in osteoclast precursor cells, and the RANKL/RANK axis may serve an important role in the differentiation of osteoclasts (24). Phospholipase Cγ (PLCγ), MAP kinases and Akt are triggered via the binding of RANKL to RANK. Activated PLCγ subsequently mediates the expression of osteoclast-specific genes through downstream factors (25).

The present study established a M-CSF + RANKL-induced osteoclast model, which was characterized by TRAP-positive staining, regular and intact F-actin rings and vigorous resorption activity, as described previously (19). The concentration of $[Ca^{2+}]_i$ varies in the process of osteoclast differentiation, and CaMKII kinase participates in osteoclast differentiation (18). Based on these data, the major role of the Ca^{2+} signaling pathway, which is involved in osteoclast differentiation and activation, was of interest. Therefore, whether the CaMKs inhibitor KN93 affected the differentiation and activation of osteoclasts was additionally investigated. The present study indicated that in the M-CSF + RANKL-induced osteoclast system, KN93 inhibited the differentiation of osteoclasts from their precursors, weakened the resorption capacity of mature osteoclasts and caused disassembly of the cytoskeletal structure. Concomitantly, KN93 downregulated the M-CSF + RANKL-induced increase in $[Ca^{2+}]_i$ concentration in RAW264.7 cells and altered the expression levels of the key genes TRAP, MMP-9 and Cathepsin K, and the key transcription factors NFATc1, c-Fos and c-Jun, which are associated with osteoclast differentiation and activation.

NFATc1 is a major osteoclastogenic transcription factor, which is critical for osteoclast terminal differentiation. It is indirectly activated by RANKL. RANK and its costimulatory receptors, namely immunoreceptor tyrosine-based activation motif proteins, coordinate to evoke PLCγ. Subsequently, inositol-1,4,5-trisphosphate (IP3), which is produced by

PLCγ, acts on IP3-sensitive Ca^{2+} channels, which are located on the surface of the endoplasmic reticulum. This give rise to Ca^{2+} excretions from the endoplasmic reticulum and intracellular Ca^{2+} levels increase rapidly in a short time period. Subsequently, calcineurin is activated, and thereby NFATc1 is stimulated and translocated to the nucleus (26). NFATc1 binds to the osteoclast-specific gene promoter region and promotes gene expression. Eventually, the osteoclast differentiation and activation properties are attributed to the osteoclast-specific gene expression (27-29). Ca^{2+} is a secondary messenger, which is mediated by Ca^{2+}-binding proteins, including calmodulin. Following transient increases in $[Ca^{2+}]_i$, Ca^{2+} interacts with calmodulin and undergoes a conformational change, which leads to the activation of CaMKs and the phosphatase calcineurin (26).

CaMKs act via the Ca^{2+}-CaMK-cyclic AMP-responsive element-binding protein (CREB) pathway and the downstream factor AP-1 in order to regulate the early stages of osteoclast differentiation (7). Concomitantly, activated CaMKs activate the ERK-MAPK signaling pathway in order to mediate the differentiation and activation of osteoclasts (18). KN93 is an inhibitor of CaMKs, and a previous study demonstrated that KN93 inhibited the activation of CaMKs in differentiated osteoclasts (18). KN93 decreased the number of TRAP-positive multinuclear cells (14). However, to the best of our knowledge, a detailed and comprehensive investigation has not been conducted to date.

TRAP staining is one of the most frequently used methods to distinguish the differentiation degree of osteoclasts. The results of the present study indicated that KN93 markedly inhibited the M-CSF + RANKL-induced osteoclastogenesis. These data were in accordance with a previous study (14). Additionally, KN93 restricted the activation of M-CSF + RANKL-induced RAW264.7 cells, which manifested in weak bone resorption ability and inhibited the formation of an intact F-actin ring. Healthy F-actin rings are considered to be crucial for osteoclast bone eroding capacity (21). In addition, the property of resorbing mineralized calcium apatite and/or carbonate substrates including bone, dentin and nacre is the most reliable criterion for the identification of osteoclast function (30). During osteoclastogenesis, Ca^{2+} oscillation is long-lasting, which may ensure the sustained induction of NFATc1 autoamplification. Therefore, intracellular Ca^{2+} is a crucial factor in osteoclastogenesis (26).

NFATc1 is activated by sustained and low Ca^{2+} activation (31), and a low Ca^{2+} threshold with regard to the constructive stimulation of transcription factors is decreased by Ca^{2+} oscillations (32,33). Long-lasting Ca^{2+} oscillation is considered to contribute to the prolonged nuclear localization of NFATc1 and ensures its sustained transcriptional activation (34). This process is required for cell terminal differentiation, including the differentiation of osteoclasts (34). In the present study, $[Ca^{2+}]_i$ levels in M-CSF + RANKL induced RAW 264.7 cells were decreased by KN93. KN93 may downregulate $[Ca^{2+}]_i$ levels and inhibit Ca^{2+} oscillation, therefore leading to an inhibition of osteoclast differentiation.

The product of TRAP gene expression is considered to be the phenotypic marker of differentiated osteoclasts (35). In addition, TRAP serves a pivotal role in the process of osteoclast bone resorption (36). Previously, the mechanism of osteoclastic bone resorption activity has been investigated more clearly. Mineralized bone matrix degradation primarily includes two processes, namely disintegration of crystalline hydroxyapatite and dissolution of organic matrix proteolytic activity (37). Carbonic anhydrase II is primarily responsible for the process of inorganic matrix degradation and the maintenance of the normal intracellular pH in the resorption area between the osteoclast and the bone matrix (38,39). Subsequently, proteolytic enzymes of the cysteine proteinase family, including Cathepsin K and the MMPs family are activated for the organic matrix degradation (40). In the present study, KN93 inhibited the expression of TRAP, MMP-9 and Cathepsin K, which demonstrated that KN93 mediated osteoclast formation and function at the molecular level. KN93 may exert its effects via the Ca^{2+}/calmodulin-dependent protein kinase signaling pathway. As aforementioned, NFATc1 localizes in the nucleus and regulates the expression of osteoclast-specific genes, including TRAP, Cathepsin K, MMP-9, osteoclast-associated receptor and calcitonin receptor.

AP-1 is crucial for osteoclastogenesis and consists of 3 protein family members, namely Fos (c-Fos, FosB, Fra-1, Fra-2), Jun (c-Jun, JunB, JunD), and activating transcription factor (ATF; ATFa, ATF2, ATF4, B-ATF) (41). Notably, c-Fos in the Fos family contributes to osteoclastogenesis to a major extent. The expression of c-Fos is inhibited by CaMKs and CREB (13,26). During osteoclastogenesis, the Jun family members may replace each other (42). During the differentiation of the osteoclasts, NFATc1 is activated by c-Fos, and the sensitization of the Ca^{2+}-Calcineurin-NFATc1 pathway is critical for this process (43). In the present study, western blot analysis suggested that KN93 decreased the levels of NFATc1, p-C-Jun and p-C-Fos during the process of osteoclastogenesis. Therefore, we hypothesize that KN93 negatively regulates osteoclastogenesis via the Ca^{2+}/calmodulin-dependent protein kinase signaling pathway.

Apart from KN93, there are other potential factors associated with the regulation of osteoclast differentiation and activation, including the mitogen-activated protein kinase pathway inhibitors SP600125, U0126 and SB203580, which will be the focus of subsequent investigations.

Taken collectively, the data from the present study suggest that KN93 inhibited the formation of TRAP-positive multinucleated cells, restricted the shaping of F-actin rings and decreased the resorption activity of osteoclasts. Additional analyses indicated that KN93 may act through the Ca^{2+}/calmodulin-dependent protein kinase signaling pathway, which regulates osteoclastogenesis. The data also demonstrated that KN93 decreased the concentration of $[Ca^{2+}]_i$, the expression levels of osteoclast-specific genes and the protein levels of critical transcription factors in the M-CSF + RANKL-induced osteoclast model.

To the best of our knowledge, the present study demonstrated for the first time that KN93, an inhibitor of CaMKs, may directly affect the differentiation and activation of osteoclasts via the Ca2+/calmodulin-dependent protein kinase signaling pathway. Additional studies are required to elucidate the detailed mechanisms of these processes. The results therefore suggested that KN93 may represent a promising therapeutic agent for the treatment of diseases associated with abnormal osteoclast activity, such as osteoporosis and osteopetrosis.

Acknowledgements

Not applicable.

Funding

This study was supported by the Project of Natural Science Foundation of Anhui Province (grant no., 1508085QH172), the Natural Science Research Project of the Universities in Anhui (grant nos., KJ2017A225 and KJ2017A237), the Natural Science Foundation of the Bengbu Medical College (grant no. BYKY1614ZD) and the National Training Programs of the Innovation and Entrepreneurship for Undergraduate (grant nos. 201410367029 and 201610367004).

Availability of data and materials

The datasets used and/or analysed during the current study are available from the corresponding author on reasonable request.

Authors' contributions

FX cultured the cells, helped to design the study, analysed and interpreted the results, and was a major contributor in the writing of the manuscript. DN and WS performed the MTT assay and tartrate-resistant acid phosphatase staining. QY, WW and BT conducted the osteoclast resorption activity assay and (F)-actin staining. ZL, DZ and YM performed the intracellular Ca^{2+} concentration quantification and reverse transcription-quantification polymerase chain reaction. CL, XL, SY and SXu performed the western blot analysis. YF and XSun cultured the cells. CC provided experimental ideas, analysed and interpreted the results, and was a major contributor in the writing of the manuscript. All authors read and approved the final manuscript.

Ethics approval and consent to participate

Not applicable.

Patient consent for publication

Not applicable.

Competing interests

The authors declare that they have no competing interests.

References

1. Kikuta J and Ishii M: Intravital bone imaging: osteoclast. Clin Calcium 28: 211-216, 2018 (In Japanese).
2. Verma SK, Leikin E, Melikov K, Gebert C, Kram V, Young MF, Uygur B and Chernomordik LV: Cell-surface phosphatidylserine regulates osteoclast precursor fusion. J Biol Chem 293: 254-270, 2018.
3. Cafiero C, Gigante M, Brunetti G, Simone S, Chaoul N, Oranger A, Ranieri E, Colucci S, Pertosa GB, Grano M and Gesualdo L: Inflammation induces osteoclast differentiation from peripheral mononuclear cells in chronic kidney disease patients: Crosstalk between the immune and bone systems. Nephrol Dial Transplant 33: 65-75, 2018.
4. Tanaka S, Nakamura I, Inoue J, Oda H and Nakamura K: Signal transduction pathways regulating osteoclast differentiation and function. J Bone Miner Metab 21: 123-133, 2003.
5. Blair HC, Robinson LJ and Zaidi M: Osteoclast signalling pathways. Biochem Biophys Res Commun 328: 728-738, 2005.
6. Del Fattore A, Teti A and Rucci N: Osteoclast receptors and signaling. Arch Biochem Biophys 473: 147-160, 2008.
7. Seales EC, Micoli KJ and McDonald JM: Calmodulin is a critical regulator of osteoclastic differentiation, function, and survival. J Cell Biochem 97: 45-55, 2006.
8. Berridge MJ, Bootman MD and Roderick HL: Calcium signalling: Dynamics, homeostasis and remodelling. Nat Rev Mol Cell Biol 4: 517-529, 2003.
9. Wagner E: Functions of AP1 (Fos/Jun) in bone development. Ann Rheum Dis 61: ii40-ii42, 2002.
10. Takayanagi H, Kim S, Koga T, Nishina H, Isshiki M, Yoshida H, Saiura A, Isobe M, Yokochi T, Inoue J, *et al*: Induction and activation of the transcription factor NFATc1 (NFAT2) integrate RANKL signaling in terminal differentiation of osteoclasts. Dev Cell 3: 889-901, 2002.
11. Linseman DA, Bartley CM, Le SS, Laessig TA, Bouchard RJ, Meintzer MK, Li M and Heidenreich KA: Inactivation of the myocyte enhancer factor-2 repressor histone deacetylase-5 by endogenous Ca(2+)/calmodulin-dependent kinase II promotes depolarization-mediated cerebellar granule neuron survival. J Biol Chem 278: 41472-41481, 2003.
12. Yao CH, Zhang P and Zhang L: Differential protein and mRNA expression of CaMKs during osteoclastogenesis and its functional implications. Biochem Cell Biol 90: 532-539, 2012.
13. Sato K, Suematsu A, Nakashima T, Takemoto-Kimura S, Aoki K, Morishita Y, Asahara H, Ohya K, Yamaguchi A, Takai T, *et al*: Regulation of osteoclast differentiation and function by the CaMK-CREB pathway. Nat Med 12: 1410-1416, 2006.
14. Chang EJ, Ha J, Huang H, Kim HJ, Woo JH, Lee Y, Lee ZH, Kim JH and Kim HH: The JNK-dependent CaMK pathway restrains the reversion of committed cells during osteoclast differentiation. J Cell Sci 121: 2555-2564, 2008.
15. Bone HG, McClung MR, Roux C, Recker RR, Eisman JA, Verbruggen N, Hustad CM, DaSilva C, Santora AC and Ince BA: Odanacatib, a cathepsin-K inhibitor for osteoporosis: A two-year study in postmenopausal women with low bone density. J Bone Miner Res 25: 937-947, 2010.
16. Stoch S and Wagner J: Cathepsin K inhibitors: A novel target for osteoporosis therapy. Clin Pharmacol Ther 83: 172-176, 2007.
17. Missbach M, Jeschke M, Feyen J, Müller K, Glatt M, Green J and Susa M: A novel inhibitor of the tyrosine kinase Src suppresses phosphorylation of its major cellular substrates and reduces bone resorption in vitro and in rodent models in vivo. Bone 24: 437-449, 1999.
18. Fu YX, Gu JH, Wang Y, Yuan Y, Liu XZ, Bian JC and Liu ZP: Involvement of the Ca^{2+} signaling pathway in osteoprotegerin inhibition of osteoclast differentiation and maturation. J Vet Sci 16: 151-156, 2015.
19. Fu YX, Gu JH, Zhang YR, Tong XS, Zhao HY, Yuan Y, Liu XZ, Bian JC and Liu ZP: Osteoprotegerin influences the bone resorption activity of osteoclast. Int J Mol Med 31: 1411-1417, 2013.
20. Livak KJ and Schmittgen TD: Analysis of relative gene expression data using real-time quantitative PCR and the 2(-delta delta C(t)) method. Methods 25: 402-408, 2001.
21. Ono T and Nakashima T: Recent advances in osteoclast biology. Histochem Cell Biol 149: 325-341, 2018.
22. Pixley FJ and Stanley ER: CSF-1 regulation of the wandering macrophage: Complexity in action. Trends Cell Biol 14: 628-638, 2004.
23. Ross FP and Teitelbaum SL: avb3 and macrophage colony-stimulating factor: Partners in osteoclast biology. Immunol Rev 208: 88-105, 2005.
24. Arai F, Miyamoto T, Ohneda O, Inada T, Sudo T, Brasel K, Miyata T, Anderson DM and Suda T: Commitment and differentiation of osteoclast precursor cells by the sequential expression of c-Fms and receptor activator of nuclear factor kappaB (RANK) receptors. J Exp Med 190: 1741-1754, 1999.
25. Lacey DL, Timms E, Tan HL, Kelley MJ, Dunstan CR, Burgess T, Elliott R, Colombero A, Elliott G, Scully S, *et al*: Osteoprotegerin ligand is a cytokine that regulates osteoclast differentiation and activation. Cell 93: 165-176, 1998.
26. Negishi-Koga T and Takayanagi H: Ca^{2+}-NFATc1 signaling is an essential axis of osteoclast differentiation. Immunol Rev 231: 241-256, 2009.

27. Lorenzo J, Horowitz M and Choi Y: Osteoimmunology: Interactions of the bone and immune system. Endocr Rev 29: 403-440, 2008.
28. Zeng X, Zhang Y, Wang S, Wang K, Tao L, Zou M, Chen N, Xu J, Liu S and Li X: Artesunate suppresses RANKL-induced osteoclastogenesis through inhibition of PLCγ1-Ca^{2+}-NFATc1 signaling pathway and prevents ovariectomy-induced bone loss. Biochem Pharmacol 124: 57-68, 2017.
29. Soysa NS, Alles N, Aoki K and Ohya K: Osteoclast formation and differentiation: An overview. J Med Dent Sci 59: 65-74, 2012.
30. Saltel F, Chabadel A, Bonnelye E and Jurdic P: Actin cytoskeletal organisation in osteoclasts: A model to decipher transmigration and matrix degradation. Eur J Cell Biol 87: 459-468, 2008.
31. Dolmetsch RE, Lewis RS, Goodnow CC and Healy JI: Differential activation of transcription factors induced by Ca^{2+} response amplitude and duration. Nature 386: 855-858, 1997.
32. Dolmetsch RE, Xu K and Lewis RS: Calcium oscillations increase the efficiency and specificity of gene expression. Nature 392: 933-936, 1998.
33. Tomida T, Hirose K, Takizawa A, Shibasaki F and Iino M: NFAT functions as a working memory of Ca^{2+} signals in decoding Ca^{2+} oscillation. EMBO J 22: 3825-3832, 2008.
34. Koga T, Matsui Y, Asagiri M, Kodama T, De Crombrugghe B, Nakashima K and Takayanagi H: NFAT and Osterix cooperatively regulate bone formation. Nat Med 11: 880-885, 2005.
35. Hofbauer LC, Neubauer A and Heufelder AE: Receptor activator of nuclear factor-kappaB ligand and osteoprotegerin: Potential implications for the pathogenesis and treatment of malignant bone diseases. Cancer 92: 460-470, 2001.
36. Price CP, Kirwan A and Vader C: Tartrate-resistant acid phosphatase as a marker of bone resorption. Clin Chem 41: 641-643, 1995.
37. Vaananen HK, Zhao H, Mulari M and Halleen JM: The cell biology of osteoclast function. J Cell Sci 113: 377-381, 2000.
38. Lehenkari P, Hentunen TA, Laitala-Leinonen T, Tuukkanen J and Väänänen HK: Carbonic anhydrase II plays a major role in osteoclast differentiation and bone resorption by effecting the steady state intracellular pH and Ca^{2+}. Exp Cell Res 242: 128-137, 1998.
39. Teitelbaum SL, Tondravi MM and Ross FP: Osteoclasts, macrophages, and the molecular mechanisms of bone resorption. J Leuk Biol 61: 381-388, 1997.
40. Kusano K, Miyaura C, Inada M, Tamura T, Ito A, Nagase H, Kamoi K and Suda T: Regulation of matrix metalloproteinases (MMP-2, -3, -9, and -13) by interleukin-1 and interleukin-6 in mouse calvaria: Association of MMP induction with bone resorption. Endocrinology 139: 1338-1345, 1998.
41. Wagner EF and Eferl R: Fos/AP-1 proteins in bone and the immune system. Immunol Rev 208: 126-140, 2005.
42. Ikeda F, Nishimura R, Matsubara T, Tanaka S, Inoue J, Reddy SV, Hata K, Yamashita K, Hiraga T, Watanabe T, *et al*: Critical roles of c-Jun signaling in regulation of NFAT family and RANKL-regulated osteoclast differentiation. J Clin Invest 114: 475-484, 2004.
43. Takayanagi H: The role of NFAT in osteoclast formation. Ann N Y Acad Sci 1116: 227-237, 2007.